



## Atmospheric "Super Test Beam" for the Pierre Auger Observatory

L. WIENCKE<sup>1</sup>, FOR THE PIERRE AUGER COLLABORATION<sup>2</sup> AND A. BOTTS<sup>1</sup>, C. ALLAN<sup>1</sup>, M. CALHOUN<sup>1</sup>, B. CARANDE<sup>1</sup>, M. COCO<sup>1,5</sup>, J. CLAUS<sup>1</sup>, L. EMMERT<sup>1</sup>, S. ESQUIBEL<sup>1</sup>, L. HAMILTON<sup>1</sup>, T.J. HEID<sup>1</sup>, F. HONECKER<sup>1,3</sup>, M. IARLORI<sup>4</sup>, S. MORGAN<sup>1</sup>, S. ROBINSON<sup>1</sup>, D. STARBUCK<sup>1</sup>, J. SHERMAN<sup>1</sup>, M. WAKIN<sup>5</sup>, O. WOLF<sup>1</sup>

<sup>1</sup> Colorado School of Mines, Department of Physics, 1523 Illinois St., Golden CO, USA

<sup>2</sup> Observatorio Pierre Auger, Av. San Martin Norte 304, 5613 Malargüe, Argentina

<sup>3</sup> Karlsruhe Institute of Technology (KIT), 76131 Karlsruhe, Germany

<sup>4</sup> CETEMPS and INFN, Dep. di Fisica Università Degli Studi dell'Aquila, via Vetoio, I-67010, L'Aquila, Italy

<sup>5</sup> Colorado School of Mines, Division of Engineering, 1500 Illinois St., Golden CO, USA

(Full author list: [http://www.auger.org/archive/authors\\_2011\\_05.html](http://www.auger.org/archive/authors_2011_05.html))

[auger\\_spokespersons@fnal.gov](mailto:auger_spokespersons@fnal.gov)

**Abstract:** We present results from 200 hours of operation of an atmospheric super test beam system developed for the Pierre Auger Observatory. The approximate optical equivalence is that of a 100 EeV air shower. This new system combines a Raman backscatter LIDAR receiver with a calibrated pulsed UV laser system to generate a test beam in which the number of photons in the beam can be determined at ground level and as a function of height in the atmosphere where high energy air showers develop. The data have been recorded simultaneously by the Raman receiver and by a single mirror optical cosmic ray detector that tested the new system by measuring the side-scattered laser light across a horizontal distance of 39 km. The new test beam instrument will be moved from the R&D location in southeast Colorado to the Pierre Auger Observatory location in Argentina to effect a major upgrade of the central laser facility.

**Keywords:** Atmosphere, LIDAR, Pierre Auger Observatory, Calibration, Raman Scattering

## 1 Introduction

The Pierre Auger Observatory uses the atmosphere as a giant calorimeter to measure properties of the highest energy particles known to exist. Test beams of particles with these extreme energies (1-100 EeV) do not exist. However light scattered out of UV laser beams directed into the atmosphere from the Central and eXtreme Laser Facilities (CLF [1] & XLF) generate tracks that are recorded by the Auger Observatory fluorescence detector (FD) [2] telescopes that also record tracks from extensive air showers. There is an approximate effective optical equivalence between a 5 mJ UV laser track and that of a 100 EeV air shower.

Atmospheric clarity, specifically the aerosol optical depth profile,  $\tau(z, t)$ , is the largest and most variable calibration term, especially for the highest energy air showers. The method to obtain  $\tau(z, t)$  that was pioneered by HiRes [3] and extended to the Auger Observatory uses FD measurements of side-scattered light from UV laser pulses [4] [5]. The relatively large light collecting power of the telescopes means that relatively few laser pulses are required. These pulses also provide a means to monitor detector calibration, performance, and aperture [6].

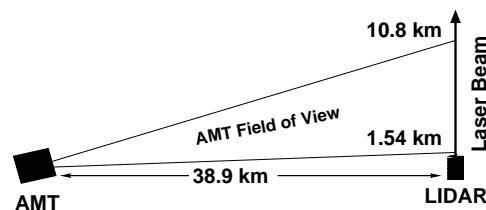


Figure 1: Geometrical arrangement, viewed from the side, of the laser and the two independent optical detectors.

To improve detector monitoring and  $\tau(z, t)$  measurements, an upgrade is planned for the CLF. This will add a Raman LIDAR receiver, replace the flash lamp laser with a solid state laser, add an automated beam calibration system [8] as used at the XLF, and improve critical infrastructure.

Key components for the upgrade have been tested at the Pierre Auger North R&D site [9] in Southeast Colorado. Data collected have been used to measure  $\tau(z, t)$  by two independent methods: elastic side scattering and inelastic (Raman) backscattering from  $N_2$  molecules. The arrangement of instruments (Fig. 1) includes the solid state laser that generates a vertical pulsed beam (355 nm 7 ns pulse width), the collocated LIDAR receiver and a simplified FD

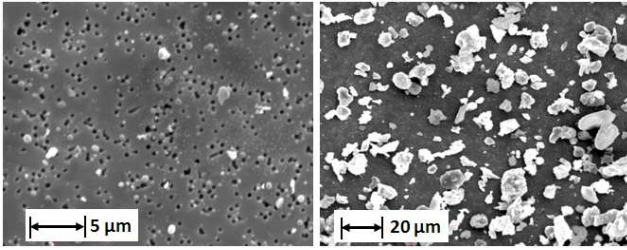


Figure 2: Scanning electron images of aerosols sampled at ground level at the Pierre Auger Observatory [10] (left: 2.5  $\mu\text{m}$  filter right: 10.0  $\mu\text{m}$  filter).

telescope 38.9 km distant. Dubbed the atmospheric monitoring telescope (AMT), this instrument records side scattered light from the laser in the same way that the Auger Observatory FD telescopes record light from the CLF and the XLF in Argentina. Data collected also include temperature, pressure and humidity profiles recorded by 27 radiosonde weather balloons launched from the LIDAR site during 2009 to 2011.

## 2 The Raman LIDAR

In measuring  $\tau(z, t)$  with elastically scattered laser light an inherent ambiguity is encountered. The measured quantity, i.e. the amount of light reaching the detector at a particular time bin (height) depends on several unknowns. These include the fraction of light transmitted to the scattering region, the fraction of light scattered in the direction of the detector by the molecular component and aerosols at the particular height, and the fraction of light transmitted back to the detector. The transmission terms can be combined if the atmosphere is assumed to be horizontally uniform, or if the receiver and laser are collocated. The molecular part of the scattering term can be determined to good accuracy from radiosonde measurements and molecular scattering theory. However the aerosol scattering term can not be modeled well because aerosol particles span a wide range of sizes and irregular shapes [10] (Fig. 2) and these properties typically vary with height.

Raman LIDARs evade this ambiguity by measuring light Raman scattered by  $\text{N}_2$  molecules. The Raman scattering cross section for  $\text{N}_2$  is well understood. The  $\text{N}_2$  density profile can be derived from radiosonde data or through the Global Data Assimilation System (GDAS) [14] [15]. Over the past few decades, Raman LIDAR has become the standard method to measure  $\tau(z, t)$ .

The Raman LIDAR receiver used in these tests features a 50 cm diameter  $f/3$  parabolic mirror pointing vertically beneath a UV transmitting window and motorized roof hatch. A liquid light guide couples the reflected light from the mirror focus to a three channel receiver (Fig. 3). Dichroic beam splitters direct this light onto 3 photomultiplier tubes (PMTs) that are located behind narrow band optical filters. These isolate the three scattered wavelengths of in-

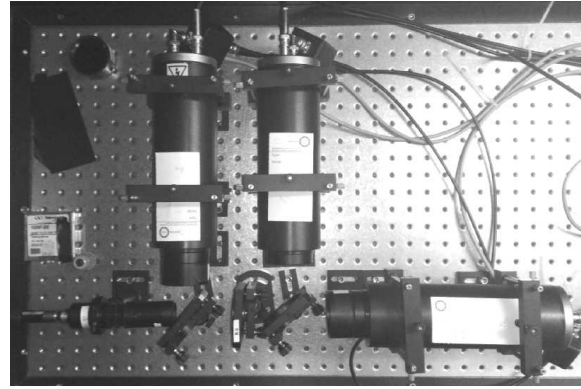


Figure 3: The three channel LIDAR receiver. Light reflected from the parabolic mirror (not shown) enters via liquid light guide seen near the lower left corner of this picture.

terest: 355 nm (Elastic scattering), 386.7 nm (Raman  $\text{N}_2$  backscattering), and 407.5 nm (Raman  $\text{H}_2\text{O}$  backscattering). The data acquisition system uses fast photon counting (250 MHz) modules. The LIDAR receiver and solid state UV laser were deployed 15 km south of Lamar, Colorado.

## 3 The AMT detector

The AMT (Fig. 4) is a modified HiRes II type telescope. The 3.5  $\text{m}^2$  mirror, camera, photomultiplier tube assemblies, and UV filter are all housed in a custom-built shelter with a roll-up door across the aperture. For these tests, the central 4 columns of  $1^\circ$  pixels were instrumented. The AMT is mounted on four concrete posts and aligned so that the vertical laser track passed near the center of the field of view (FOV). The FOV at the vertical laser spans 1.54 to 10.8 km above the ground. A precipitation and ultrasonic wind sensor ensure the door was closed during rainy or windy conditions. The AMT is pointed toward the north so that direct sunlight could not damage the camera if the door is open during the day. The door and field of view can be observed remotely through a network video camera.

The PMTs were gain sorted prior to installation. Data from a temperature controlled UV LED system at the mirror center and from a vertical nitrogen laser scanned across the field of view were used to flat field and debug the camera. During routine nightly operation, the relative calibration was monitored using the LED system.

The readout of the PMT current is performed by pulse shaping and digitization system electronics that are also implemented in the High Elevation Auger Telescope (HEAT) [11] [12] extension to the Auger Observatory. The sampling period is 50 ns. The readout is triggered externally, either by pulses from the UV LED system, or from a GPS device [13]. The laser is also triggered by the same model GPS device. The AMT GPS pulse output is delayed by 130  $\mu\text{s}$  to allow for light travel time between the two instruments.

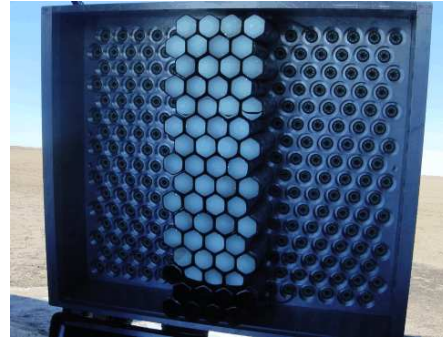


Figure 4: The remotely operated Atmospheric Monitoring Telescope (left) and its camera (right) with the central 4 columns instrumented. A rectangular UV transmitting filter (not shown) normally covers the camera surface.

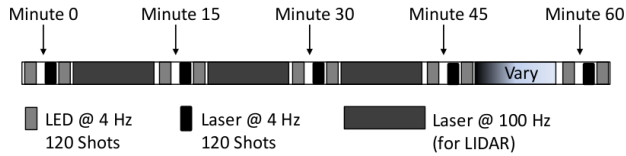


Figure 5: The hourly sequence of operations.

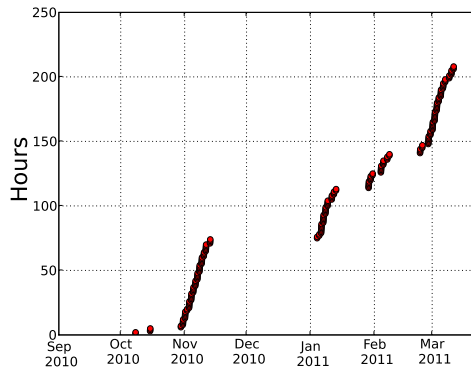


Figure 6: Accumulation of data when the AMT and the Raman LIDAR operated on the same hour

## 4 Operations and Data Analysis

The AMT, LIDAR, laser and various subsystems are all operated under computer control. Their nightly operation is sequenced by automation scripts initiated on moonless nights from the Colorado School of Mines campus. Operation and data collection are then monitored remotely by collaborators in Colorado, Germany, and Italy. The hourly sequence (Fig. 5) interleaves sets of 200 laser shots at 4 Hz for AMT measurements, sets of 120 UV LED shots for AMT relative calibration, and 12 minute sets of 100 Hz laser shots for LIDAR measurements. Between October 2010 and March 2011, more than 200 hours of data have been accumulated for which the AMT and LIDAR measured laser light during the same hour (Fig. 6).

The Raman LIDAR was benchmarked against the European LIDAR network EARLINET [7] prior to shipment

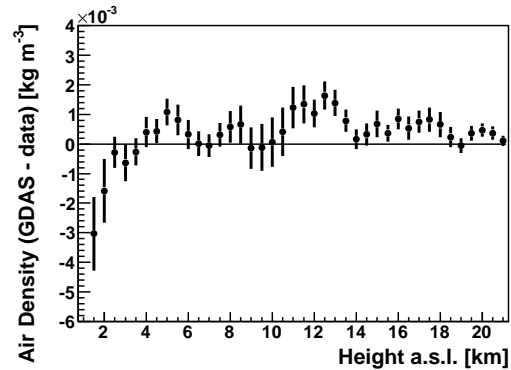


Figure 7: Average difference in atmospheric density as determined from the GDAS model and measured from 27 radiosondes launches.

from Italy. The algorithm used in this benchmark was also used to retrieve aerosol profiles in Colorado from the  $N_2$  channel. The  $N_2$  density was obtained from the GDAS model. The model agreed well with the radiosonde data collected at the site (Fig. 7).

The measurement of  $\tau(z, t)$  from the AMT data used the data normalized retrieval algorithm adapted from the version used in Argentina to obtain  $\tau(z, t)$  from FD measurements of vertical CLF laser pulses. Two reference nights were selected in the Colorado sample. The analysis included corrections for variations in the laser output and in the relative calibration of the AMT. Systematic errors of 3% were assigned to these terms and an equivalent error was assigned for the choice of reference night.

## 5 Results

A correlation is observed between the two independent measurements of aerosol optical depth (Fig. 8). Periods of obvious cloud were removed from this analysis. The smallest differences in absolute terms are observed during lower aerosol conditions, i.e.  $\tau(4.5 \text{ km}) < 0.05$ . Horizontal non-uniformity of the aerosol distribution across the 39 km between detectors can be expected to contribute to the broad-

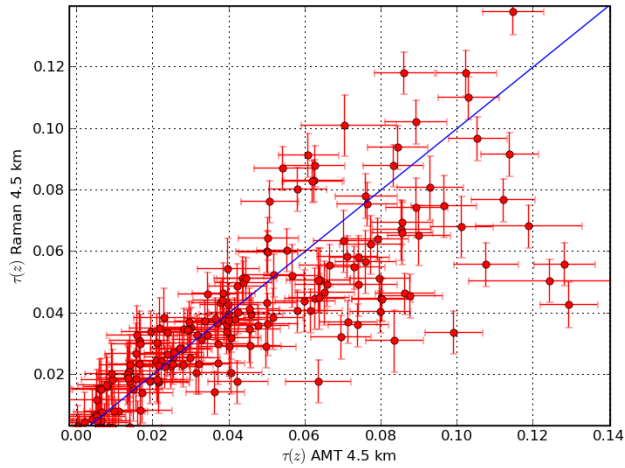


Figure 8: Comparison between the vertical aerosol optical depth at 4.5 km as measured by the AMT and the Raman LIDAR systems.

ening of the correlation under hazier conditions. Further analysis is in progress. We note this work represents the first systematic comparison between these methods as applied to astroparticle detectors.

## 6 Targeted applications of the CLF upgrade

Because of the relatively small size of the Raman scattering cross section, thousands of laser shots are needed to accumulate sufficient photon statistics. This has potential to interfere significantly with FD operation. However, a number of specific physics targets have been identified for which one set of Raman LIDAR measurements per night is expected to provide a valuable supplement to current methods.

1. Systematically compare the aerosol optical depth profiles measured by the Raman LIDAR and by the side-scatter method. This comparison is motivated by the elongation rate for hybrid data that suggests the particle composition may transition to heavier primaries above 10 EeV.
2. Better identify periods of extremely low aerosol concentration to reduce uncertainty in the data normalized aerosol analysis.
3. Use the super test beam to crosscheck the end-to-end photometric calibration of the FD which sets the energy scale for the observatory. The difference between the energy spectra measured by the Auger Observatory and by other experiments could be explained by a systematic difference in energy scales.
4. Precision measurement of aerosols shortly after detection of especially interesting air showers. The Raman receiver will make an independent precision measurement of the aerosol optical depth profile and

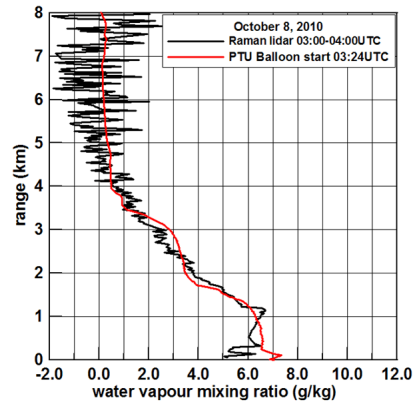


Figure 9: Water vapor profile measured by a radiosonde (smoother line) and by the LIDAR on the same evening.

water vapor profile. An example water vapor profile as measured by the LIDAR and by a radiosonde is shown in Fig. 9.

## References

- [1] B. Fick *et al.* JINST, 2006, **1** 11003.
- [2] The Pierre Auger Collaboration, Nucl. Instr. And Meth., 2010, **A620**, 227-251.
- [3] HiRes Collaboration, Astropart. Phys., 2006, **25**, 74-83.
- [4] L. Valore for the Pierre Auger Collaboration, Proc. 31st ICRC, Łódź, Poland, 2009 (arXiv:0906.2358[astro-ph]).
- [5] The Pierre Auger Collaboration, Astropart. Phys, 2010 **33**, 108-129.
- [6] The Pierre Auger Collaboration, Astropart. Phys., 2011, **A34**, 368-381.
- [7] [www.earlinet.org](http://www.earlinet.org).
- [8] L. Wiencke, F. Arqueros, J. Compton, M. Monasor, D. Pilger and J. Rosado, Proc. 31st ICRC, Łódź, Poland, 2009 (arXiv:1105.4016 [astro-ph]).
- [9] F. Sarazin for the Pierre Auger Collaboration, contribution 0944 in these proceedings.
- [10] M. Micheletti (private communication).
- [11] M. Kleifges for the Pierre Auger Collaboration, Proc. 31st ICRC, Łódź, Poland, 2009 (arXiv:0906.2354[astro-ph]).
- [12] H.J. Mathes for the Pierre Auger Collaboration, contribution 0761 in these proceedings.
- [13] J. Smith, J. Thomas, S. Thomas, and L. Wiencke, Proc. 30th ICRC, Mérida, México 2007, **5** 997-1000. US Patent 7,975,160.
- [14] NOAA Air Resources Laboratory (ARL), Global Data Assimilation System (GDAS1) Archive Information, Tech. rep. 2004. URL <http://ready.arl.noaa.gov/gdas1.php>
- [15] M. Will for the Pierre Auger Collaboration, contribution 0339 in these proceedings.